

# Driving mechanisms behind the various phases in manganese perovskites revealed by Mn 2p resonance photoemission

A. Sekiyama,<sup>1,\*</sup> H. Fujiwara,<sup>1</sup> A. Higashiya,<sup>1</sup> S. Imada,<sup>1</sup> H. Kuwahara,<sup>2</sup> Y. Tokura,<sup>3</sup> and S. Suga<sup>1</sup>

<sup>1</sup>*Department of Material Physics, Graduate School of Engineering Science, Osaka University, Toyonaka, Osaka 560-8531, Japan*

<sup>2</sup>*Department of Physics, Sophia University, Tokyo 102-0094, Japan*

<sup>3</sup>*Department of Applied Physics, University of Tokyo, Tokyo 113-8656, Japan*

(Dated: November 6, 2018)

Unusual temperature and doping dependence of the Mn 3d spectral functions of manganese perovskites  $\text{Nd}_{1-x}\text{Sr}_x\text{MnO}_3$  has been revealed by the high-resolution Mn 2p–3d resonance photoemission. The temperature-dependent spectra cannot be explained by any theoretical model currently under debate, while showing evidence for a microscopic and dynamic phase segregation. The experimental results strongly suggest that the competition of both the dynamical and static Jahn-Teller effects with ferromagnetic ordering at high and low temperatures, respectively, is responsible for the actual electronic states.

PACS numbers: 75.30.-m, 79.60.-i, 71.30.+h, 75.50.Cc

Manganese perovskites have extensively been studied regarding colossal magnetoresistance (CMR) [1, 2, 3] and charge-ordering [4] from both scientific and engineering viewpoints. Their electronic states have fundamentally been understood by the so-called double-exchange (DE) mechanism [5, 6] for a long time. In the last decade, it has been recognized that a dynamical Jahn-Teller (JT) effect induced by a local lattice distortion also plays a substantial role. [7, 8] Nowadays there are many theoretical models and calculations for the manganites, which well reproduce the temperature dependence of the resistivity [2, 3] and the optical conductivity. [9, 10, 11] Meanwhile the Mn 3d spectral functions and their temperature dependence obtained from angle-integrated photoemission are thought to be crucial for the test of these models, namely, to see whether these models really explain the Mn 3d spectral functions.

The photoemission data so far accumulated on manganites [12, 13, 14, 15, 16, 17, 18, 19] could not satisfactorily check the applicability of the theoretical models since most of the valence-band photoemission spectra have been obtained with low-energy light sources. The low-energy photoemission ( $h\nu \lesssim 120$  eV) spectra of three-dimensional transition-metal (TM) oxides mainly reflect the O 2p electronic states and moreover surface electronic structures, which might deviate strongly from the bulk TM 3d states, because of the relatively large ratio of the O 2p/TM 3d photoionization cross sections [20] and a short photoelectron mean free path [21] ( $\lambda < 5$  Å, bulk contribution of  $< 30\%$ ). The Mn 2p–3d resonance photoemission ( $h\nu \sim 640$  eV with  $\lambda \sim 13$  Å, leading to a predominant bulk contribution of  $\sim 60\%$ ) is promising for a more adequate discussion of the Mn 3d bulk electronic states and their temperature dependence since the Mn 3d spectral weight is selectively and drastically enhanced at the Mn 2p absorption threshold as shown in Fig. 1(a). The Mn 3d enhancement is much weaker and the bulk

sensitivity is much less at the Mn 3p–3d resonance excitation,  $h\nu \sim 50$  eV. [12] However, it has been difficult for a long time to obtain the temperature-dependent Mn 3d spectra at the 2p–3d resonance with high resolution, because both photon flux of conventional synchrotron light sources and energy resolution of soft x-ray monochromators have been insufficient. It is inevitable to use a high-brilliance and high photon flux synchrotron light source in order to obtain the Mn 2p–3d resonance photoemission spectra with such a high energy resolution and good statistics as presented here. This has allowed us for the first time to observe the detailed temperature dependence of the electronic structures of manganites. In this Letter, we show a unified picture of the driving mechanisms leading to the various aspects of the 3d electronic states in the manganese perovskites.

Here we report on the system  $\text{Nd}_{1-x}\text{Sr}_x\text{MnO}_3$  with  $x = 0.40, 0.47, 0.50$ . The compounds with  $x = 0.40$  and  $0.47$  undergo a paramagnetic insulator (PI)-to-ferromagnetic metal (FM) transition at  $T_c \sim 290$  and  $275$  K, respectively, where the FM state is stable down to the lowest temperatures below  $T_c$ . [22] The PI-FM transition is also seen for  $x = 0.50$  ( $T_c \sim 255$  K), while this compound is a charge-ordered insulator (COI) below  $T_{\text{COI}} \sim 160$  K. [4] The photoemission measurements were performed at BL25SU in SPring-8. [23] The overall energy resolution was set to  $\sim 100$  meV. The base pressure was about  $4 \times 10^{-8}$  Pa. For the temperature-dependent measurements, clean surfaces were obtained by fracturing the single crystalline samples *in situ* at 280–300 K in the PI phase. Then the spectra were measured at the resonance-maximum ( $h\nu = 643$  eV) on cooling. A possible Auger contribution is clarified to be negligible at  $h\nu = 643$  eV within the energy region from  $E_F$  to  $\sim 3$  eV. The surface cleanliness was confirmed before and after the measurements. We also checked that the Mn 3d spectra at low temperatures with fracture at low temperatures were very similar to

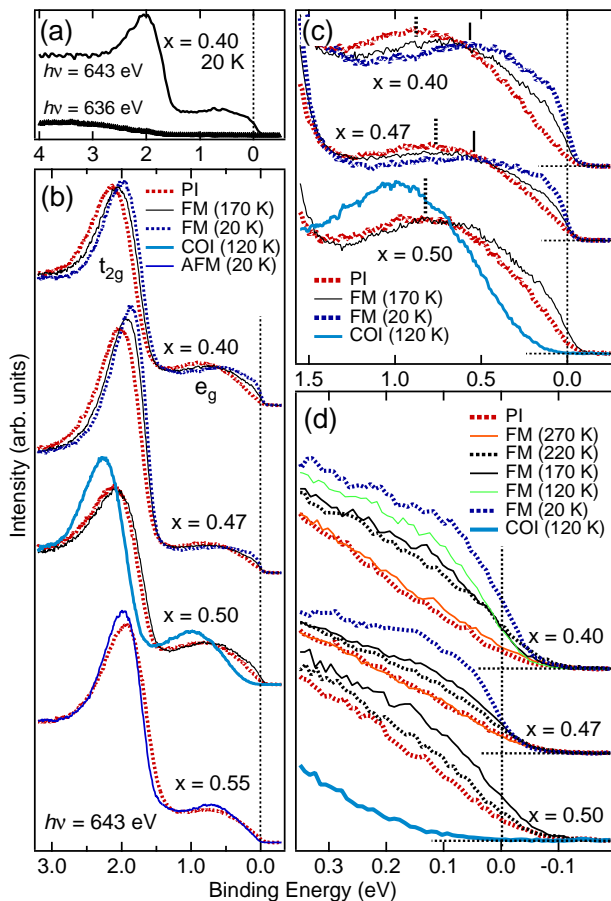


FIG. 1: Mn  $2p - 3d$  resonance photoemission spectra of  $\text{Nd}_{1-x}\text{Sr}_x\text{MnO}_3$  ( $x = 0.40, 0.47, 0.50, 0.55$ ). (a) Mn  $2p - 3d$  resonance-maximum ( $h\nu = 643$  eV) and off-resonance ( $h\nu = 636$  eV) photoemission spectra of  $\text{Nd}_{0.6}\text{Sr}_{0.4}\text{MnO}_3$  measured at 20 K in the FM phase. The spectral intensity has been normalized to the photon flux. (b) High-resolution Mn  $2p - 3d$  resonance-maximum spectra representing the Mn  $3d$  contributions in the PI (300 K for  $x = 0.40$  and  $0.47$ , 280 K for  $x = 0.50$  and 260 K for  $x = 0.55$ ), FM (20 and 170 K for  $x = 0.40$  and  $0.47$ , 170 K for  $x = 0.50$ ) and COI (120 K for  $x = 0.50$ ) phases. The spectrum for  $x = 0.55$  measured in the antiferromagnetic metal (AFM, 20 K) phase is also added for comparison. (c) Same as (b), but focused on the  $e_g$  spectral weight. (d) Detailed temperature dependence of the Mn  $3d$  spectral weights near  $E_F$  for  $x = 0.40, 0.47$  and  $0.50$  in the PI, FM and COI (120 K for  $x = 0.50$ ) phases. The spectral weights at different temperatures in (b)-(d) have been normalized to the integrated intensity from  $E_F$  to  $\sim 4$  eV for each compound.

these results.

The temperature dependence of the Mn  $2p - 3d$  on-resonance spectra (Mn  $3d$  spectra hereafter) of  $\text{Nd}_{1-x}\text{Sr}_x\text{MnO}_3$  is summarized in Figs. 1(b)-(d). The  $t_{2g}$ -derived electronic states appear as a strong peak near 2.0 eV. The spectral weight from  $E_F$  to  $\sim 1.5$  eV originates dominantly from the  $e_g$  states. These qualitative spectral features are in agreement with previous re-

sults [13, 17, 19] Surprisingly, however, the Mn  $3d$  spectral line shapes change gradually with temperature not only in the  $e_g$  region but also in the  $t_{2g}$  region. Such spectral changes over a range of several eV within the same phase are very unusual. The  $t_{2g}$  peak shifts gradually towards  $E_F$  for  $x = 0.40$  and  $0.47$  by about 0.15 eV between 300 and 20 K. On the contrary, the  $t_{2g}$  as well as the  $e_g$  components shift abruptly to higher binding energies concomitant with the opening of a clear energy gap of the order of 100 meV (Fig. 1(d)) for  $x = 0.50$  as a result of the FM-COI transition. As shown in Fig. 1(b), the gradual  $t_{2g}$  peak shift for  $x = 0.40$  and  $0.47$  is not observed for  $\text{Nd}_{0.45}\text{Sr}_{0.55}\text{MnO}_3$  ( $x = 0.55$ ), which undergoes a transition from the PI to antiferromagnetic metal (AFM) at 220 K. [24] These results indicate that the gradual  $t_{2g}$  peak shift towards  $E_F$  with decreasing temperature for  $x = 0.40$  and  $0.47$  is characteristic of the PI-FM transition.

A broad peak at 0.8-0.9 eV is observed in the PI phase as indicated by dashed bars in Fig. 1(c). We emphasize that this structure survives even in the FM phase at high temperatures while it is remarkably suppressed at 20 K for  $x = 0.40$  and  $0.47$  accompanied by a change of the spectral shape. Namely, another broad peak is seen at 0.5-0.6 eV as indicated by solid bars in Fig. 1(c). According to detailed measurements [see Fig. 1(d)], the intensity from  $E_F$  to  $\sim 0.3$  eV is gradually enhanced with decreasing temperature in the FM phase. A clear Fermi cut-off is seen at low temperatures for  $x = 0.40$  and  $0.47$ .

To date, there has been a controversy whether the spectral function changes with temperature within the FM phase based on the low-energy photoemission data. [13, 14, 15] Our results clearly show that the Mn  $3d$  spectral functions in both the  $t_{2g}$  and the  $e_g$  regions *do* change within the FM phase. Furthermore, there are two additional significant features in our spectra. One is that the spectra from 0.3 eV to  $E_F$  remains essentially unchanged across the PI-FM transition [see Fig. 1(d)], in clear contrast to the remarkable change of the spectra across the FM-COI transition for  $x = 0.50$ . The other is that the photoemission intensity at  $E_F$  is distinctly finite even in the PI phase, which has never been seen before in the low-energy photoemission data. [13, 14, 15, 16, 18] We emphasize that the observed finite intensity at  $E_F$  in the PI phase is intrinsic and cannot be reproduced by an instrumental resolution broadening of any plausible spectral line shape assumed to become zero intensity at  $E_F$ . [25] The finite intensity at  $E_F$  indicates that the compounds in the PI phase are neither simple band insulators nor Mott insulators as induced by an on-site Coulomb interaction between the Mn  $3d$  electrons. It is thus found that the  $3d$  electron correlation effects alone, which themselves are strong as previously pointed out, [12, 14, 17] cannot account for the PI-FM transition in the manganites.

We now turn to a discussion of the existing theoret-

ical models against this anomalous temperature dependence of the Mn  $3d$  spectral functions. The key issues of our data are summarized as follows: (a) finite intensity at  $E_F$  even in the PI phase, (b)  $t_{2g}$  peak shift with temperature in the FM phase, (c) presence of a peak at 0.8-0.9 eV in the PI phase, and (d) gradual intensity reduction of this peak and the appearance of another peak at 0.5-0.6 eV with decreasing temperature in the FM phase. Although the calculations based on the DE mechanism [26, 27] are not contradictory to (a), they cannot predict the  $e_g$ -derived broad peak away from  $E_F$  at all, namely, fail to explain (c) and (d). The dynamical JT model [7, 8] and a model including the orbital degrees of freedom [28, 29] seem to fairly explain (a) and (c) since they show the broad-peak structure away from  $E_F$ . However, such a peak is hardly shifted with temperature according to these models, which is contradictory to (d). In addition, these models are not likely to explain (b) because the center of gravity in the calculated  $e_g$  spectral weights is hardly shifted with temperature. To conclude, all theoretical approaches mentioned above are still insufficient even for a qualitative explanation of the temperature dependence of the Mn  $3d$  spectra. A further elaborated theoretical model is required to explain our experimental findings.

In order to understand the temperature-dependent spectral functions as much as possible from experimental viewpoint, we have tried to reproduce the spectra for  $x = 0.40$  and  $0.47$  measured at 120, 170, 220, and 270 K in the FM phase by a linear combination of the spectra at 20 K in the FM phase and those at 300 K in the PI phase. As shown in Fig. 2 for  $x = 0.40$ , the linear combination of the spectra well reproduces the Mn  $3d$  spectra in both the  $e_g$  and the  $t_{2g}$  regions at intermediate temperatures. This analysis indicates that the spectra in the FM phase still include the spectral component of the PI phase, whose weight is gradually reduced with decreasing temperature. Such a scenario that a dynamic and microscopic phase segregation grows in the FM region with increasing temperature, as has been proposed from inelastic neutron scattering on  $\text{La}_{0.7}\text{Ca}_{0.3}\text{MnO}_3$ , [30] is the most likely story to explain our data.

In the following we show a unified picture, which explains the various electronic phases in the manganites. We focus now on the  $e_g$  spectral weight and its temperature and doping dependence. The spectral shape in the PI phase is essentially similar for different  $x$  as shown in Fig. 1(b) and 1(c). In the ground states at the lowest temperature, on the other hand, the peak in the  $e_g$  region becomes more prominent for  $x = 0.50$  (COI) and  $0.55$  (AFM) at higher binding energies compared with the PI phase, while it becomes broader for  $x = 0.40$  (FM) and  $0.47$  (FM) in the sense that the  $e_g$  states extend above  $E_F$  (remember that the clear Fermi cut-off is seen at low temperatures). This tendency corresponds well with the static JT distortion which is stronger for

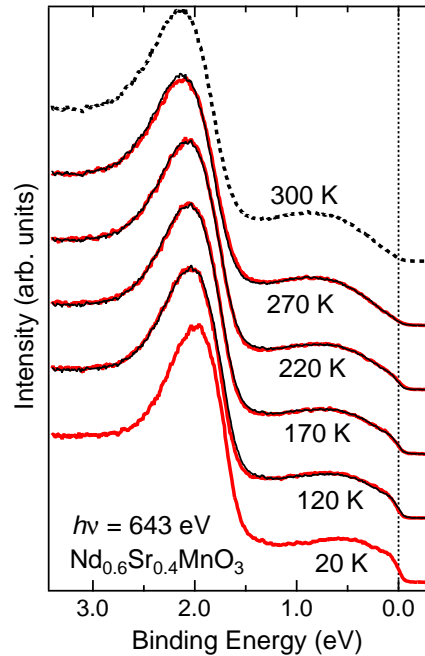


FIG. 2: Detailed temperature dependence of the Mn  $2p - 3d$  resonance photoemission spectra of  $\text{Nd}_{0.6}\text{Sr}_{0.4}\text{MnO}_3$ . The red solid lines show the spectra in the FM phase while the black dashed line is in the PI phase at 300 K. Proper linear combinations of the two experimental spectra at 20 K and 300 K are shown by the black thin solid lines at intermediate temperatures, which can well reproduce the experimental results. In the linear combinations, the relative contributions of the 20 K spectrum are 68, 54, 43 and 7 % at 120, 170, 220 and 270 K, respectively, with an accuracy of  $\pm 7$  %. We have also successfully reproduced the temperature-dependent Mn  $3d$  spectra of  $\text{Nd}_{0.53}\text{Sr}_{0.47}\text{MnO}_3$  in the FM phase (not shown) by the linear combination of the spectra at 20 K and 300 K, where the contributions of the spectrum at 20 K are 50, 29 and 4 % at 170, 220 and 270 K, respectively.

$x = 0.50$  and  $0.55$  than for  $x = 0.40$  and  $0.47$  at low temperatures. [4, 22, 24] It is thought that the  $e_g$  electron partially occupies the lower JT split band and hence provides more spectral weight at higher binding energies in the  $e_g$  region. Accordingly the observed temperature dependence and the dynamic and microscopic phase segregation scenario are well understood as follows: The static JT distortion (i.e., the degree of freedom in the  $e_g$  orbitals) mainly controls the  $3d$  electronic states in the ground states at low temperatures. In particular, the completely developed FM phase without phase segregation can be realized at low temperatures for the compositions  $x = 0.40$  and  $0.47$  in which the static JT distortion is weak, while the FM ordering is suppressed for  $x = 0.50$  and  $0.55$  where the JT distortion is strong. In the PI phase near room temperature, on the other hand, the dynamical JT effect governs the  $3d$  electronic states irrespective of both  $x$  and the strength of the static JT distortion at low temperatures. The dynamical JT effect

weakens gradually with decreasing temperature below  $T_c$ . Then the amount of the FM phase grows correspondingly for  $0.40 \leq x \leq 0.50$ . In this way, the dynamical and static JT effects hinder the FM ordering in the manganites at high and low temperatures, respectively.

Finally we point out a close relation between the CMR and the dynamic phase segregation. The CMR effect is not notable near the phase boundary between the PI and FM states for  $\text{Nd}_{1-x}\text{Sr}_x\text{MnO}_3$  ( $x = 0.40-0.50$ ) compared with that between the FM and COI states for  $\text{Nd}_{0.5}\text{Sr}_{0.5}\text{MnO}_3$ . From the above discussion, we conclude that the dynamic phase segregation originating from the gradually changed dynamical JT effect with temperature plays an important role in reducing the CMR at the PI-FM transition. Namely, in such a situation as the dynamical JT effect is strong in the PI phase and abruptly suppressed at the PI-FM transition, CMR would be remarkable.

In conclusion, we have clearly observed the temperature dependence of the high-resolution Mn  $2p - 3d$  resonance photoemission spectra of  $\text{Nd}_{1-x}\text{Sr}_x\text{MnO}_3$  in the PI and FM phases as well as evidence for the microscopic and dynamic phase segregation. It is clarified that  $\text{Nd}_{1-x}\text{Sr}_x\text{MnO}_3$  in the PI phase are found to be neither a band insulator nor a Mott insulator. Although our results cannot be well explained by any available model, we propose a unified picture to interpret the experimental results. The  $3d$  electronic states are mainly controlled by the static JT effect at low temperatures whereas the dynamical JT effect governs the electronic states near room temperature.

We thank K. Noda, K. Konoike, T. Satonaka, S. Kasai, A. Yamasaki, A. Irizawa, M. Tsunekawa, and the staff of SPring-8, especially T. Muro, Y. Saitoh, and T. Matsushita for supporting the experiments. This work was supported by a Grant-in-Aid for COE Research from the Ministry of Education, Culture, Sports, Science and Technology (MEXT), Japan. AS acknowledges the support from the Kurata foundation. The photoemission measurements were performed under the approval of the Japan Synchrotron Radiation Research Institute (2001A0129-NS-np, 2003A0593-NS1-np).

- [1] R. von Helmolt *et al.*, Phys. Rev. Lett. **71**, 2331 (1993).
- [2] Y. Tokura *et al.*, J. Phys. Soc. Jpn. **63**, 3931 (1994).
- [3] A. Urushibara *et al.*, Phys. Rev. B **51**, 14103 (1995).
- [4] H. Kuwahara *et al.*, Science **270**, 961 (1995).
- [5] C. Zener, Phys. Rev. **82**, 403 (1951).
- [6] P. W. Anderson, H. Hasegawa, Phys. Rev. **100**, 675 (1955).
- [7] A. J. Millis, B. I. Shraiman, R. Mueller, Phys. Rev. Lett. **77**, 175 (1996).
- [8] A. J. Millis, R. Mueller, B. I. Shraiman, Phys. Rev. B **54**, 5405 (1996).
- [9] S. G. Kaplan *et al.*, Phys. Rev. Lett. **77**, 2081 (1999).
- [10] Y. Okimoto *et al.*, Phys. Rev. B **55**, 4206 (1997).
- [11] M. W. Kim *et al.*, Phys. Rev. Lett. **89**, 016403 (2002).
- [12] T. Saitoh *et al.*, Phys. Rev. B **51**, 13942 (1995).
- [13] J. -H. Park *et al.*, Phys. Rev. Lett. **76**, 4215 (1996).
- [14] D. D. Sarma *et al.*, Phys. Rev. B **53**, 6873 (1996).
- [15] A. Chainani *et al.*, Phys. Rev. B **56**, R15513 (1997).
- [16] J. -H. Park *et al.*, Nature **392**, 794 (1998).
- [17] A. Sekiyama *et al.*, Phys. Rev. B **59**, 15528 (1999).
- [18] Y. -D. Chuang *et al.*, Science **292**, 1509 (2001).
- [19] J. -S. Kang *et al.*, Phys. Rev. B **68**, 012410 (2003).
- [20] J. J. Yeh, I. Lindau, At. Data Nucl. Data Tables **32**, 1 (1985).
- [21] S. Tanuma, C. J. Powell, D. R. Penn, Surf. Sci. **192**, L849 (1987).
- [22] R. Kajimoto *et al.*, Phys. Rev. B **60**, 9506 (1999).
- [23] Y. Saitoh *et al.*, Rev. Sci. Instrum. **71**, 3254 (2000).
- [24] H. Kuwahara *et al.*, Phys. Rev. Lett. **82**, 4316 (1999).
- [25] As for the PI phase for  $x = 0.40-0.55$ , the spectra in a binding energy region from 0.05 to  $\sim 0.5$  eV can be fairly reproduced by a power-law of the binding energy ( $E_B$ ), i.e.,  $|E_B|^\alpha$  where  $\alpha \sim 0.7-1$  and the spectral weight is originally zero at  $E_F$ . However, the spectral weight at and above  $E_F$  cannot be quantitatively explained by broadening the power-law spectral weight with the experimental resolution ( $\sim 100$  meV). From these facts, it is surely concluded that the observed finite spectral weight at  $E_F$  is intrinsic in the PI phase.
- [26] A. Kubo, J. Phys. Soc. Jpn. **33**, 929 (1972).
- [27] N. Furukawa, J. Phys. Soc. Jpn. **64**, 3164 (1995).
- [28] S. Yunoki, A. Moreo, Phys. Rev. B **58**, 6403 (1998).
- [29] S. Yunoki, A. Moreo, E. Dagatto, Phys. Rev. Lett. **81**, 5612 (1998).
- [30] J. Zhang *et al.*, Phys. Rev. Lett. **86**, 3823 (2001).

---

\* sekiyama@mp.es.osaka-u.ac.jp

---

\* sekiyama@mp.es.osaka-u.ac.jp